HHS Public Access

Author manuscript

Nat Chem. Author manuscript; available in PMC 2020 July 08.

Published in final edited form as:

Nat Chem. 2019 July ; 11(7): 644–652. doi:10.1038/s41557-019-0278-x.

De novo macrocyclic peptides that specifically modulate Lys48-linked ubiquitin chains

Mickal Nawatha[1], **Joseph Rogers**[2], **Steven M. Bonn**[3], **Ido Livneh**[4], **Betsegaw Lemma**[3], **Sachitanand M. Mali**[1], **Ganga B. Vamisetti**[1], **Hao Sun**[1], **Beatrice Bercovich**[4], **Yichao Huang**[2], **Aaron Ciechanover**[4], **David Fushman**[3], **Hiroaki Suga**[2], **Ashraf Brik**[1]

[1]Schulich Faculty of Chemistry, Technion-Israel Institute of Technology, Haifa 3200008, Israel.

[2]Department of Chemistry, Graduate School of Science, The University of Tokyo, 7-3-1 Hongo, Bunkyo-ku, Tokyo 113-0033, Japan.

[3]Department of Chemistry and Biochemistry, Center for Biomolecular Structure and Organization, University of Maryland, College Park, MD 20742, USA.

[4]The Rappaport Faculty of Medicine and Research Institute, Technion-Israel Institute of Technology, Haifa 31096, Israel.

Abstract

A promising approach in cancer therapy is to find ligands that directly bind ubiquitin (Ub) chains. However, finding molecules capable of tightly and specifically binding Ub chains is challenging given the range of Ub polymer lengths and linkages and their subtle structural differences. Here, we use total chemical synthesis of proteins to generate highly homogenous Ub chains for screening against trillion-member macrocyclic peptide libraries (RaPID system). *De novo* cyclic peptides were found that can bind tightly and specifically to K48-linked Ub chains, confirmed by NMR studies. These cyclic peptides protected K48-linked Ub chains from deubiquitinating enzymes and prevented proteasomal degradation of Ub-tagged proteins. The cyclic peptides could enter cells, inhibit growth and induce programmed cell death, opening new opportunities for therapeutic intervention. This highly synthetic approach, with both protein target generation and cyclic peptide discovery performed *in vitro*, will make other elaborate post-translationally modified targets accessible for drug discovery.

Ashraf Brik (abrik@technion.ac.il).

Author Contributions: J.M.R and M.N contributed equally to this work. J.M.R. carried out cyclic peptide discovery RaPID system, SPR assays, data analysis and co-wrote the paper. M.N. assisted in the chemical synthesis of cyclic peptides, carried out *in vitro* and cellular assays and co-wrote the paper. I.L. carried out confocal microscopy assay and assisted with the cellular studies. S.M.B., B.L. synthesized isotope-labeled Ub chains, conducted the NMR studies, and assisted writing the paper. S.M.M. assisted in chemical synthesis of the ubiquitin chains. G.B. assisted in the synthesis of cyclic peptides. H. Sun prepared the δ-mercaptolysine used in the ubiquitin chain synthesis. B.B. assisted the design of the *in vitro* proteasomal degradation assay. D.F. designed and supervised the NMR studies, carried out data analysis and assisted in the writing of the manuscript and SI. Yichao Huang performed additional SPR studies against K11- and K63-linked Ub chains. A.C. assisted in the design of the confocal microscopy assay, *in vitro* and cellular studies. H. Suga supervised the RaPID study and assisted in the writing of the paper. A.B. designed and supervised the entire project and the writing of the paper.

Competing Interests: The authors declare no competing interests.

Data Availability: The data that support the findings of this study are available from the corresponding author upon reasonable request.

Graphical Abstract

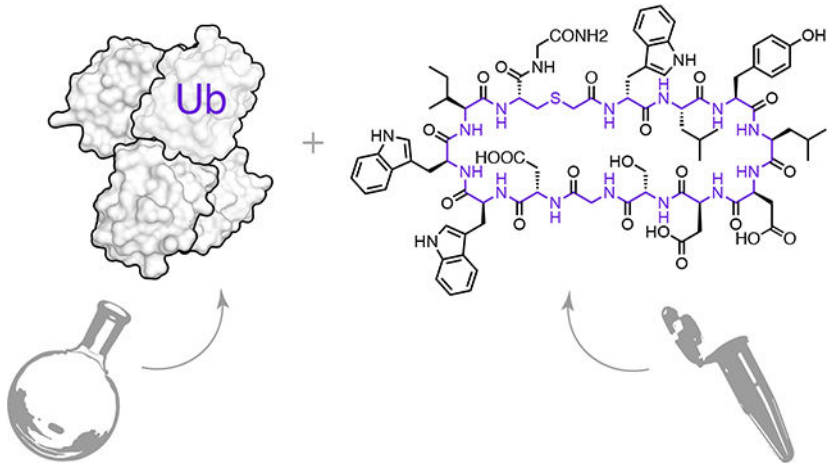

Introduction

The initial step in ubiquitin (Ub) signaling is the modification of a protein substrate by Ub or polyUb chains[1,2]. This is achieved by the collaborative action of three enzymes, the E1, E2 and E3 ligases[3]. In ubiquitination, an isopeptide bond is formed between the C-terminus of a Ub molecule and a lysine residue from the protein substrate. PolyUb chains are then made by repeated isopeptide or amide bond formation, linking any of the seven lysines, or the N-terminus, of the last Ub in the chain and to the C-terminus of a new Ub[4,5]. Interestingly, Ub chains of different linkage types signal for different biological functions, likely due to their unique conformations which allows for distinct recognition by cellular proteins. The most studied polyUbs are the K48-linked chains, which are known to adopt a compact structure and label their protein substrate for proteasomal degradation[6,7]. Ubiquitination is a reversible process and a family of enzymes known as deubiquitinases (DUBs) cleave Ub from polyUb chains, or remove polyUb entirely[5,8].

Ubiquitination is a major post-translational modification affecting many aspects of cell biology[9,10]. Several tumor suppressors or oncogenes are involved in ubiquitination or deubiquitination pathways, making the Ub system an excellent target for cancer therapy[11]. For example, the ubiquitin-proteasome system (UPS) has proven to be a valid target for anticancer drug development, as exemplified by the approval of the small molecule Bortezomib for the treatment of multiple myeloma and mantle cell lymphoma[12,13,14]. Drugs such as Bortezomib interfere with protein degradation by inhibiting the UPS proteolysis machinery[15,16], whereas other strategies target different components of Ub signaling, such ubiquitination itself or the action of DUBs, with success yet to be translated to useful therapies[5,17].

Another promising approach is targeting the Ub chain itself. In this regard, the small molecules ‘ubistatins’ fortuitously emerged from a chemical genetic screen, and were found to bind monomeric Ub as well as K48-linked chains, and thereby impair recognition by the

proteasome and inhibit protein degradation[18]. However, ubistatins have weak (sub-μM to μM) binding and poor chain specificity[19].

Targeting Ub chains of particular lengths and linkages could control different cellular processes. However, this represents a significant challenge for molecular recognition, given the number of possible Ub chains[4] and the often subtle differences in their structure and dynamics[20,21]. Yet, we have envisioned that this could be achieved using macrocyclic peptides, which can tightly interact with proteins using extended interfaces[22], similar to natural protein-protein interactions, but at the same time are small enough to emulate drug-like *in vivo* properties of small molecules[23].

There are powerful methods to discover *de novo* binding peptide sequences, such as the RaPID system (Random non-standard Peptides Integrated Discovery). In the RaPID system, *in vitro* translation is modified to use reprogrammed genetic codes[24], including nonproteinogenic amino acids that allow for spontaneous peptide macrocyclization[25]. RaPID can generate huge, trillion-member libraries of DNA-tagged cyclic peptides[26, 27]. Panning these libraries for target engagement, followed by DNA sequencing, allows for selection of highly specific, tight binding *de novo* cyclic peptide sequences.

We reasoned that the RaPID system could produce cyclic peptide ligands capable of discriminating between Ub chains. However, the success of such a selection would depend critically on the homogeneity, in length and linkage, of these target Ub polymers. This is difficult to achieve using biochemical and biological approaches for all the Ub chains. However, recently it has become possible to assemble the protein Ub and polyUb by total chemical synthesis. This allows for the construction of high-purity Ub chains, with defined lengths[28] and linkage types, including any required modifications, suitable for use as targets in these challenging selections.

By combining the RaPID system and chemical protein synthesis of Ub chains, we discover for the first time *de novo* cyclic peptides that tightly bind the K48-linked Ub chains, with great selectivity towards the chain length (mono-, di-, and tetra-Ub) and linkage type (K48 vs K63 or K11). We also report the *in vitro* effects of the selected cyclic peptide on the behavior of these Ub chains, e.g. their interaction with DUBs and the proteasome, as well as their ability to inhibit cellular protein degradation.

Results

Choice of K48-linked target

We sought to determine whether selectivity towards different Ub oligomeric forms or a particular chain linkage is possible using cyclic peptides. We chose K48-linked Ub chains as targets for *de novo* cyclic peptide discovery, as chemical compounds that can bind K48-linked Ub have biological and therapeutic significance. In particular, the degradation of specific cellular proteins by the 26S proteasome, controlled using K48-linked polyUb tags, determines whether a cell proliferates or dies[29]. Cancer cells use degradation of certain proteins e.g. p53, Bax and p27[30–32], to avoid the triggering of apoptosis. Therefore, K48-

linked polyUb-binding cyclic peptides may elevate the levels of these short-lived proteins and might selectively restore apoptosis in these cells[31,33,11].

Total chemical synthesis of biotin tagged K48-linked Ub chains

We applied our chemical toolbox to construct K48-linked Ub chains suitable for RaPID selection. This consists of orthogonally protected δ-mercaptolysine[34], solid phase peptide synthesis (SPPS) of Ub monomers (modified as required), coupled with isopeptide chemical ligation and desulfurization to prepare mono Ub (Ub_1), di-Ub ($^{K48}Ub_2$) and tetra-Ub ($^{K48}Ub_4$) chains[35]. The N-terminus of each distal Ub was further modified with biotin, to facilitate immobilization to a solid support (Fig. 1a). Highly homogenous Ub chains were obtained which could be reconstituted into folded proteins, and bound to streptavidin (Supplementary Figs 1–3).

Discovery of *de novo* cyclic peptides for K48 Ub chains

The chemically synthesized Ub chains, biotin-$^{K48}Ub_2$ and biotin-$^{K48}Ub_4$, were used as targets for two separate RaPID selections (Fig. 1b). The initial cyclic peptide libraries contained ~10^{13} unique sequences, with 8–12 random amino acids per peptide. After the first round of selection an additional step was introduced, binding to biotin-Ub_1, to remove cyclic peptides that might use Ub_1 as the main recognition element. Deep sequencing of the DNA library after each round showed that a small number of peptide sequences, and their variants, came to dominate the library by round 4 (Fig. 1c, Supplementary Fig. 4). Rounds 2–4 were repeated and produced a similar pattern of enrichment (Supplementary Fig. 4). In the $^{K48}Ub_2$ selections the libraries became dominated by the same two sequences, **Ub2i** and **Ub2ii** (Fig. 1c, Supplementary Fig. 4). In the $^{K48}Ub_4$ selections, many of the top peptides had appreciable sequence identity to **Ub2i** (Supplementary Fig. 4); One of these high identity peptides (58 %), **Ub4i**, was chosen for further study together with a shorter, lower identity peptide (8 %), **Ub4ix** (Fig. 1c).

De novo cyclic peptides tightly bind K48-linked Ub chains

To test the binding and specificity of the **Ub2i**, **Ub2ii**, **Ub4i** and **Ub4ix** cyclic peptides, each was prepared by SPPS (Supplementary Fig. 5) for Surface Plasmon Resonance (SPR) analysis (Fig 1d). Each peptide was flowed over immobilized Ub chains: the selection targets $^{K48}Ub_2$ and $^{K48}Ub_4$, as well as Ub_1, and alternatively linked $^{K11}Ub_2$, $^{K63}Ub_2$. **Ub2i** and **Ub2ii** bound tightly to their selection target $^{K48}Ub_2$, with low-nM K_d values (40 ± 12 nM, 33 ± 8 nM, respectively, Fig 1d). However, **Ub2i** and **Ub2ii** also strongly bound the longer chain $^{K48}Ub_4$, with a low apparent K_d and an increased SPR response (Fig 1d). This is consistent with a higher stoichiometry of binding to the tetramer, which could be explained by the fact that $^{K48}Ub_2$ structure can be superimposed twice on the $^{K48}Ub_4$ crystal structure (Supplementary Fig. 6)[36].

Ub4i tightly bound its selection target $^{K48}Ub_4$, but also bound $^{K48}Ub_2$ similar to **Ub2i** and **Ub2ii**. This is perhaps unsurprising, given the high sequence identity between **Ub4i** and **Ub2i**. On the other hand, the cyclic peptide **Ub4ix** was highly specific for the K48-linked Ub tetramer: weakly binding $^{K48}Ub_2$ (> 1 μM K_d) but tightly binding to $^{K48}Ub_4$ (K_d = 6 ± 1 nM).

None of the cyclic peptides showed detectable binding to Ub_1 (Supplementary Methods). This was expected as the RaPID selection was designed to avoid recovering Ub_1 binders. More interestingly, the cyclic peptides showed marked selectivity for the K48-linkage over alternative linkages: there was no detectable binding, for any of the cyclic peptides, to either K11-linked or K63-linked di-Ub (Supplementary Methods).

Mapping of cyclic peptide/K48-linked poly-Ub interface using NMR

We then became interested in understanding the binding mode of the discovered cyclic peptides with the K48-linked Ub chains. We used NMR to confirm physical interaction between **Ub2ii** and $^{K48}Ub_2$ and to map the residues/sites involved in the peptide binding. The peptide was titrated into solution of $^{K48}Ub_2$ where either distal or proximal Ub was ^{15}N-enriched (Supplementary Fig. 7), and the binding was monitored by ^{1}H-^{15}N NMR. The titration revealed site-specific interactions with both Ub units (Figs. 2a,b and Supplementary Fig. 8). Interestingly, the NMR spectra followed a text-book example of slow exchange, where a gradual decrease in intensity of the “unbound” Ub signals was accompanied by appearance and increase of alternate (“bound”) signals. At a 1:1 molar ratio, practically all affected unbound signals vanished (Figs. 2a and Supplementary Fig. 8). This likely reflects slow off-rates, in full agreement with the SPR data (Supplementary Table S1) and strong, nM-K_d binding (Fig. 1e). By contrast, only minor spectral perturbations were observed upon addition of **Ub2ii** to mono-Ub and $^{K63}Ub_2$ (data not shown), corroborating high specificity of the peptide for $^{K48}Ub_2$.

The $^{K48}Ub_2$ sites affected by **Ub2ii** binding were mapped to residues in and around the L8-I44-V70 hydrophobic patch on both Ub units (Fig. 2b–c), indicating that the cyclic peptide intercalates between the two Ub units in $^{K48}Ub_2$. Simultaneous binding of both Ub units to the same cyclic peptide is supported by the fact that the saturation was reached at the 1:1 molar ratio indicating a 1:1 stoichiometry of the resulting Ub_2/**Ub2ii** complex. The observed interface is similar to that involved in $^{K48}Ub_2$ interactions with ubistatins[18,19] as well as K48-specific protein receptors[37]. Interestingly, despite the general symmetry between the two Ub units in Ub_2, the chemical shift perturbations (CSPs) and the directions of the signal shifts are drastically different between the distal and the proximal Ubs. Combined with the fact that only a single set of “bound” NMR signals is observed for each Ub unit, this indicates that **Ub2ii** binds $^{K48}Ub_2$ unidirectionally and in a single conformation.

Using NMR, we also monitored the interaction between **Ub4ix** and $^{K48}Ub_4$. As with $^{K48}Ub_2$/**Ub2ii**, the binding was in slow-exchange regime, and the interface was mapped primarily to the hydrophobic surface patch on each Ub unit studied (Figs. 2d,e and Supplementary Figs. 9–11). Interestingly, the most distal Ub exhibited relatively weaker spectral perturbations compared to the other units in the chain, and the disappearance of the unbound signals occurred at higher peptide concentrations than for Ub unit 3 or the proximal Ub, suggesting relatively weaker **Ub4ix** interaction with the most distal Ub in the chain. To examine if this was related to the length of the chain or the external (distal) position of the Ub unit, we performed similar binding studies for $^{K48}Ub_3$ (Supplementary Figs. 12–14). The spectral perturbations in the distal Ub of this tri-Ub were comparable with those in unit 3 of $^{K48}Ub_4$ but different from the most distal Ub in $^{K48}Ub_4$ (Figs. 2d, Supplementary Fig. 15).

Also the proximal Ub units in $^{K48}Ub_4$ and $^{K48}Ub_3$ exhibited similar patterns of residue-specific signal shifts (Supplementary Fig. 16). Together, these results suggest that the cyclic peptide **Ub4ix** primarily binds to/across the first three Ub units in $^{K48}Ub_4$. Consistent with this conclusion and the SPR results, the addition of **Ub4ix** to $^{K48}Ub_2$ caused lesser spectral perturbations than in the case of **Ub2ii** peptide at the same (1:1) molar ratio (data not shown), indicating weaker binding.

Cyclic peptide binding to Ub chains protects these chains against DUB cleavage *in vitro*.

It is possible that the binding of these cyclic peptides to Ub chains prevents their recognition by interacting proteins such as DUBs. We chose to examine the effect of these cyclic peptides on two DUBs: OTUB1[38], a K48-linkage chain specific DUB, and USP2, which cleaves most Ub chains without specificity[39], using $^{K48}Ub_2$ and $^{K48}Ub_4$ chains as substrates (Fig. 3). All peptides were able to inhibit OTUB1 with $^{K48}Ub_2$ as the substrate (Fig. 3a), at ratio of 1:1 cyclic peptide: substrate, even the weakest binding peptide **Ub4ix** was able to fully inhibit OTUB1 (Fig. 3c). This suggests that binding to Ub chains by cyclic peptides can interfere with recognition by the DUB. However, with USP2 using $^{K48}Ub_2$ as the substrate, we observed only ~40% inhibition in the presence of **Ub2i**, **Ub2ii** or **Ub4i**, and only minimal inhibition by **Ub4ix** (Fig. 3b). Excess **Ub4ix** over substrate concentration was required to completely inhibit the activity of USP2 (Fig. 3d). Using a $^{K48}Ub_4$ chain as the substrate instead, both OTUB or USP2 could cleave down to monomer Ub units, and this cleavage was inhibited in the presence of the cyclic peptides (Fig. 3e, f). However, USP2 in the presence of the cyclic peptides **Ub2i**, **Ub4ix**, and **Ub4i** could only remove the distal Ub of $^{K48}Ub_4$[40], shortening the chain to the trimer $^{K48}Ub_3$, the peptides show strong inhibition of further disassembly of the chain (Fig. 3e, f). For **Ub4ix** this can be explained by the NMR result that suggested that the cyclic peptide only weakly interacts with the distal Ub, which may be sterically accessible for cleavage by USP2. Interestingly, the same cyclic peptides did not protect $^{K63}Ub_2$ chains from USP2 cleavage, nor the structurally similar $^{K11}Ub_2$, from Cezanne cleavage[41] (Supplementary Fig. 17), highlighting the specificity of the cyclic peptides towards the K48-linkage, supporting by the NMR and SPR studies (see above) .

Cyclic peptide binding to Ub chains prevents ubiquitinated proteins from proteasomal degradation

It is possible that the binding of cyclic peptides to K48-linked Ub chains could prevent the recognition by the proteasome, and inhibit the degradation of proteins tagged with these Ub chains. To test this we incubated synthetic α-globin-$^{K48}Ub_4$ with 26S proteasome, with and without **Ub4ix**. Without **Ub4ix**, the α-globin-$^{K48}Ub_4$ substrate was degraded by the proteasome. However, with equimolar amounts of **Ub4ix** relative to α-globin-$^{K48}Ub_4$, degradation was inhibited, a similar effect to that of the direct proteasome inhibitor, MG132 (Fig. 4). Uncyclized linear **Ub4ix** showed no inhibition, highlighting the requirement of the cyclic topology for binding to Ub.

Ub4ix is able to enter into HeLa cells.

In order to assess the feasibility of using **Ub4ix** in cultured cells, we next tested whether **Ub4ix** is able to cross the cellular membrane of human cells. We synthesized **Ub4ix** labeled

with fluorescein (Fig. 5a, Supplementary Fig. 18), and used live cell imaging to monitor its entrance into HeLa cells. The uptake of labeled **Ub4ix** was apparent as early as 4 hours (Fig. 5b). Following its addition to the culture medium, with further intracellular marked accumulation, throughout the following 48 hours (Fig. 5b). Comparing the uptake of fluorescein-**Ub4ix** with fluorescein alone in three cell lines (HeLa, U2OS osteosarcoma and U87 primary glioblastoma cells), fluorescein-**Ub4ix** exhibited considerable cell permeability (Fig. 5c). In addition, we screened the cellular uptake fluorescein-**Ub4ix** compared to free fluorescein, after incubation for 16 hr (Fig. 5d). **Ub4ix** was quickly and efficiently distributed within cells, allowing tests in more representative biological models without further modification or special delivery systems.

Ub4ix activity causes accumulation of Ub-conjugates

Under basal conditions, the levels of Ub-conjugates reflect a dynamic steady state between the enzymatic tagging of Ub to proteins on the one hand, with the removal of conjugated Ub moieties by DUBs, and subsequent degradation by the proteasome, on the other. We have shown *in vitro* that the cyclic peptide **Ub4ix** can protect Ub-chains from cleavage by DUBs, and also prevent recognition by the proteasome. Both effects would be predicted to prevent degradation, and lead to the accumulation, of proteins tagged with K48-Ub chains in cells. First we confirmed that **Ub4ix** does not affect protein synthesis (Supplementary Fig. 19). Then, we monitored the cellular level of Ub-conjugates in cells upon treatment with **Ub4ix**. We were able to demonstrate a time and dose dependent elevation in Ub-conjugates following treatment with **Ub4ix**, both in its free and fluorescein labeled forms (Fig. 5e and f), a similar result to treating with the direct proteasome inhibitor MG132 (Fig. 5e and f).

In order to directly measure the effect of **Ub4ix** on proteolysis, we radiolabeled cellular proteins, followed by a chase experiment in the presence of either **Ub4ix** or the proteasome inhibitor MG132. When compared to non-treated cells, or ones treated with DMSO, protein breakdown in cells treated with **Ub4ix** was markedly reduced, a similar result to those observed in the presence of MG132 (Fig. 5g). Both agents show a dose-dependent effect on cellular protein degradation. We validated this inhibitory effect on the breakdown of proteins known to be proteasomal substrates; the proteins p27[42] and p53[43]. In the presence of the **Ub4ix**, p53 and p27 were accumulated over time, up to a similar level to those observed in the presence of MG132 (Fig. 5h).

Cyclic peptides induce apoptosis

Given that **Ub4ix** has a pronounced inhibitory effect on the UPS system, it may also be able to inhibit cell growth and induce apoptosis in cancer cells. To test this, HeLa cells were treated with each cyclic peptide, and cell growth was found to be dramatically suppressed when viability was assessed using an MTT (3-(4,5-dimethylthiazol-2-yl)-2, 5-diphenyltetrazolium bromide) assay. We noted that **Ub4ix** was the most effective in suppressing growth (Fig. 6a). The effects of the cyclic peptides on apoptosis were also evaluated using fluorescence-activated cell sorting (FACS) analysis. Intriguingly, **Ub4ix** at 10 μM exhibited clear increase in apoptosis after 24 hr and 48 hr treatment, similar to the direct proteasome inhibitor MG132 (Fig. 6b).

Discussion

We have discovered *de novo* cyclic peptides that bind tightly and specifically to K48-linked Ub chains. Ub-binding domains with a similar function exist in biology, but typically these bind with weak affinities (μM K_d values[44]), mainly to the L8-I44-V70 hydrophobic patch on the Ub surface, and display a narrower range of affinities for different Ub chain lengths and linkages. By contrast, antibodies have been discovered that can bind strongly (nM K_d), and specifically to polyUb chains by directly interacting with the isopeptide bond and its surrounding residues[45]. Surprisingly, the *de novo* macrocyclic peptides exhibit remarkably high affinity and linkage specificity like the antibodies. Yet, they interact with the hydrophobic surface of Ub frequently used by the weak-binding, poorly-selective natural Ub-binding domains. The affinity and selectivity profiles of these cyclic peptides are even more impressive given their significantly lower molecular masses relative to the protein domains and antibodies. Importantly, it is this smaller size that permits entry into cells[46].

These cyclic peptides show *in vitro* and cellular activity comparable to a potent proteasome inhibitor, and can similarly trigger apoptosis in cancer cells. However, they act through a different mechanism. By binding to Ub chains directly and strongly, they interfere with the recognition and subsequent proteasomal processing of these chains. This different mechanism may have therapeutic advantages, as it can avoid the innate and acquired resistance associated with direct proteasome inhibitors[47]: it is difficult to mutate the Ub target, given its essentiality and its short, highly conserved sequence[48]. Importantly, unlike generic Ub-binding small molecules[19], these cyclic peptides do not bind Ub_1, K11- or K63-linked Ub chains strongly or specifically. Therefore, many Ub-directed cellular processes can continue unimpeded in the presence of these cyclic peptides. Our ability to synthesize different Ub chains with various lengths and linkage types, coupled with RaPID system, could lead to the discovery of novel cyclic peptides that interfere with specific cellular responses associated with these different Ub chains, to shed light on the full range of Ub signals in health and disease.

The combination of high-fidelity total protein synthesis and the cyclic peptide discovery RaPID system has produced *de novo* ligands capable of distinguishing between subtly different oligomers of the same protein domain. The control offered by this highly synthetic, *in vitro* approach will make other elaborate, post-translationally modified targets proteins accessible for ligand discovery. In particular, other Ub chains with different linkages and lengths, ubiquitinated proteins and Ub-like conjugates can be targeted to interfere with a wide range of cellular processes[28]. These cyclic peptides will be valuable tools to understand Ub signaling in health and disease, and open new opportunities in drug discovery related to the Ub system.

Supplementary Material

Refer to Web version on PubMed Central for supplementary material.

Acknowledgments:

A. Brik holds The Jordan and Irene Tark Academic Chair. H. Sun is supported at the Technion by a Technion-Guangdong Fellowship. This work was supported by the Japan Agency for Medical Research and Development, Basic Science and Platform Technology Program for Innovative Biological Medicine (JP18am0301001) to H. Suga, and by NIH grant GM065334 to D. Fushman. J.M.R was supported by Grants-in-aid for JSPS Fellows (P13766), Joint ANR-JST grant (ANR-14-JITC-2014-003 and JST-SICORP). We thank Ananya Majumdar for help with triple-resonance NMR experiments. A.C. is supported by the Dr. Miriam and Sheldon Adelson Medical Research Foundation (AMRF), the Israel Science Foundation (ISF), the German-Israeli Foundation for Research and Development (GIF) and a Professorship funded by the Israel Cancer Research Fund (ICRF).

References

1. Glickman MH & Ciechanover A The Ubiquitin-Proteasome Proteolytic Pathway: Destruction for the Sake of Construction. Physiol. Rev 82, 373–428 (2002). [PubMed: 11917093]
2. Hersko A & Ciechanover A The ubiquitin system. Annu. Rev. Biochem 67, 425–479 (1998). [PubMed: 9759494]
3. Pickart CM Mechanisms underlying ubiquitination. Annu. Rev. Biochem 70, 503–33 (2001). [PubMed: 11395416]
4. Komander D & Rape M The Ubiquitin Code. Annu. Rev. Biochem 81, 203–229 (2012). [PubMed: 22524316]
5. Gopinath P, Ohayon S, Nawatha M & Brik A Chemical and semisynthetic approaches to study and target deubiquitinases. Chem. Soc. Rev 45, 4171–4198 (2016). [PubMed: 27049734]
6. Ikeda F & Dikic I Atypical ubiquitin chains: new molecular signals. 'Protein Modifications: Beyond the Usual Suspects' review series. EMBO Rep. 9, 536–42 (2008). [PubMed: 18516089]
7. Finley D Recognition and processing of ubiquitin-protein conjugates by the proteasome. Annu. Rev. Biochem 78, 477–513 (2009). [PubMed: 19489727]
8. Reyes-Turcu FE & Wilkinson KD Polyubiquitin binding and disassembly by deubiquitinating enzymes. Chem. Rev 109, 1495–1508 (2009). [PubMed: 19243136]
9. Huang X & Dixit VM Drugging the undruggables: exploring the ubiquitin system for drug development. Cell Res. 26, 484–498 (2016). [PubMed: 27002218]
10. Pickart CM & VanDemark AP Opening doors into the proteasome. Nat. Struct. Biol 7, 999–1001 (2000). [PubMed: 11062549]
11. Adams J The development of proteasome inhibitors as anticancer drugs. Cancer Cell 5, 417–421 (2004). [PubMed: 15144949]
12. Goldberg AL Development of proteasome inhibitors as research tools and cancer drugs. J. Cell Biol 199, 583–588 (2012). [PubMed: 23148232]
13. Groll M, Berkers CR, Ploegh HL & Ovaa H Crystal structure of the boronic acid-based proteasome inhibitor bortezomib in complex with the yeast 20S proteasome. Structure 14, 451–456 (2006). [PubMed: 16531229]
14. Richardson PG et al. (2005) Bortezomib or high-dose dexamethasone for relapsed multiple myeloma. N Engl J Med 352, 2487–2498. [PubMed: 15958804]
15. Deshaies RJ Proteotoxic crisis, the ubiquitin-proteasome system, and cancer therapy. BMC Biol. 12, 94 (2014). [PubMed: 25385277]
16. Lee DH & Goldberg AL Proteasome inhibitors : valuable new tools for cell biologists. Trends Cell Biol. 8, 397–403 (1998). [PubMed: 9789328]
17. Harrigan JA, Jacq X, Martin NM & Jackson SP Deubiquitylating enzymes and drug discovery: Emerging opportunities. Nat. Rev. Drug Discov 17, 57–77 (2018). [PubMed: 28959952]
18. Verma R et al. Ubistatins inhibit proteasome-dependent degradation by binding the ubiquitin chain. Science 306, 117–120 (2004). [PubMed: 15459393]
19. Nakasone MA et al. Structural Basis for the Inhibitory Effects of Ubistatins in the Ubiquitin-Proteasome Pathway. Structure. 25, 1839–1855 (2017). [PubMed: 29153505]
20. Ye Y et al. Ubiquitin chain conformation regulates recognition and activity of interacting proteins. Nature 492, 266–270 (2012). [PubMed: 23201676]

21. Castañeda CA et al. Linkage-specific conformational ensembles of non-canonical polyubiquitin chains. Phys. Chem. Chem. Phys 18, 5771–5788 (2016). [PubMed: 26422168]
22. Jongkees S. a. K., Hipolito CJ, Rogers JM & Suga H Model foldamers: applications and structures of stable macrocyclic peptides identified using in vitro selection. New J. Chem 39, 3197–3207 (2015).
23. Zorzi A, Deyle K & Heinis C Cyclic peptide therapeutics: past, present and future. Curr. Opin. Chem. Biol 38, 24–29 (2017). [PubMed: 28249193]
24. Goto Y, Katoh T & Suga H Flexizymes for genetic code reprogramming. Nat. Protoc 6, 779–790 (2011). [PubMed: 21637198]
25. Goto Y et al. Reprogramming the initiation event in translation for the synthesis of physiologically stable cyclic peptides. ACS Chem. Biol 3, 120–129 (2008). [PubMed: 18215017]
26. Yamagishi Y et al. Natural product-like macrocyclic N-methyl-peptide inhibitors against a ubiquitin ligase uncovered from a ribosome-expressed de novo library. Chem. Biol 18, 1562–1570 (2011). [PubMed: 22195558]
27. Jongkees SAK et al. Rapid Discovery of Potent and Selective Glycosidase-Inhibiting De Novo Peptides. Cell Chem. Biol 24, 381–390 (2017). [PubMed: 28262556]
28. Mali SM, Singh SK, Eid E & Brik A Ubiquitin signaling: chemistry. comes to the rescue. J. Am. Chem. Soc 139, 4971–4986 (2017). [PubMed: 28328208]
29. Orlowski RZ The role of the ubiquitin-proteasome pathway in apoptosis. Cell Death Differ. 6, 303 (1999). [PubMed: 10381632]
30. Maki CG, Huibregtse JM & Howley PM In vivo ubiquitination and proteasome-mediated degradation of p53. Cancer Res. 56, 2649–2654 (1996). [PubMed: 8653711]
31. Li B & Dou QP Bax degradation by the ubiquitin/proteasome-dependent pathway: involvement in tumor survival and progression. Proc. Natl. Acad. Sci. U. S. A 97, 3850–5 (2000). [PubMed: 10725400]
32. Lloyd RV et al. P27Kip1: a Multifunctional Cyclin-Dependent Kinase Inhibitor With Prognostic Significance in Human Cancers. Am. J. Pathol 154, 313–23 (1999). [PubMed: 10027389]
33. Vaziri SAJ et al. Inhibition of proteasome activity by bortezomib in renal cancer cells is p53 dependent and VHL independent. Anticancer Res. 29, 2961–2969 (2009). [PubMed: 19661301]
34. Ajish Kumar KS, Haj-Yahya M, Olschewski D, Lashuel HA & Brik A Highly efficient and chemoselective peptide ubiquitylation. Angew. Chem. Int. Ed 48, 8090–8094 (2009).
35. Bavikar SN et al. Chemical synthesis of ubiquitinated peptides with varying lengths and types of ubiquitin chains to explore the activity of deubiquitinases. Angew. Chem. Int. Ed 51, 758–763 (2012).
36. Eddins MJ, Varadan R, Fushman D, Pickart CM & Wolberger C Crystal Structure and Solution NMR Studies of Lys48-linked Tetraubiquitin at Neutral pH. J. Mol. Biol 367, 204–211 (2007). [PubMed: 17240395]
37. Varadan R, Assfalg M, Raasi S, Pickart C & Fushman D Structural determinants for selective recognition of a Lys48-linked polyubiquitin chain by a UBA domain. Mol. Cell 18, 687–698 (2005). [PubMed: 15949443]
38. Mevissen TET et al. OTU Deubiquitinases Reveal Mechanisms of Linkage Specificity and Enable Ubiquitin Chain Restriction Analysis. Cell 154, 169–184 (2013). [PubMed: 23827681]
39. Renatus M et al. Structural Basis of Ubiquitin Recognition by the Deubiquitinating Protease USP2. Structure 14, 1293–1302 (2006). [PubMed: 16905103]
40. Stanley M & Virdee S Chemical ubiquitination for decrypting a cellular code. Biochem. J 473, 1297–1314 (2016). [PubMed: 27208213]
41. Bremm A, Freund SMV & Komander D Lys11-linked ubiquitin chains adopt compact conformations and are preferentially hydrolyzed by the deubiquitinase Cezanne. Nat. Struct. Mol. Biol 17, 939–947 (2010). [PubMed: 20622874]
42. Pagano M et al. Role of the ubiquitin-proteasome pathway in regulating abundance of the cyclin-dependent kinase inhibitor p27. Science 269, 682–5 (1995). [PubMed: 7624798]
43. Devine T & Dai M-S Targeting the ubiquitin-mediated proteasome degradation of p53 for cancer therapy. Curr. Pharm. Des 19, 3248–62 (2013). [PubMed: 23151129]

44. Raasi S, Varadan R, Fushman D & Pickart CM Diverse polyubiquitin interaction properties of ubiquitin-associated domains. Nat. Struct. Mol. Biol 12, 708–714 (2005). [PubMed: 16007098]

45. Newton K et al. Ubiquitin Chain Editing Revealed by Polyubiquitin Linkage-Specific Antibodies. Cell 134, 668–678 (2008). [PubMed: 18724939]

46. Pye CR et al. Nonclassical Size Dependence of Permeation Defines Bounds for Passive Adsorption of Large Drug Molecules. J. Med. Chem 60, 1665–1672 (2017). [PubMed: 28059508]

47. Lü S & Wang J The resistance mechanisms of proteasome inhibitor bortezomib. Biomark. Res 1, 13 (2013). [PubMed: 24252210]

48. Roscoe BP, Thayer KM, Zeldovich KB, Fushman D & Bolon DNA Analyses of the effects of all ubiquitin point mutants on yeast growth rate. J. Mol. Biol 425, 1363–1377 (2013). [PubMed: 23376099]

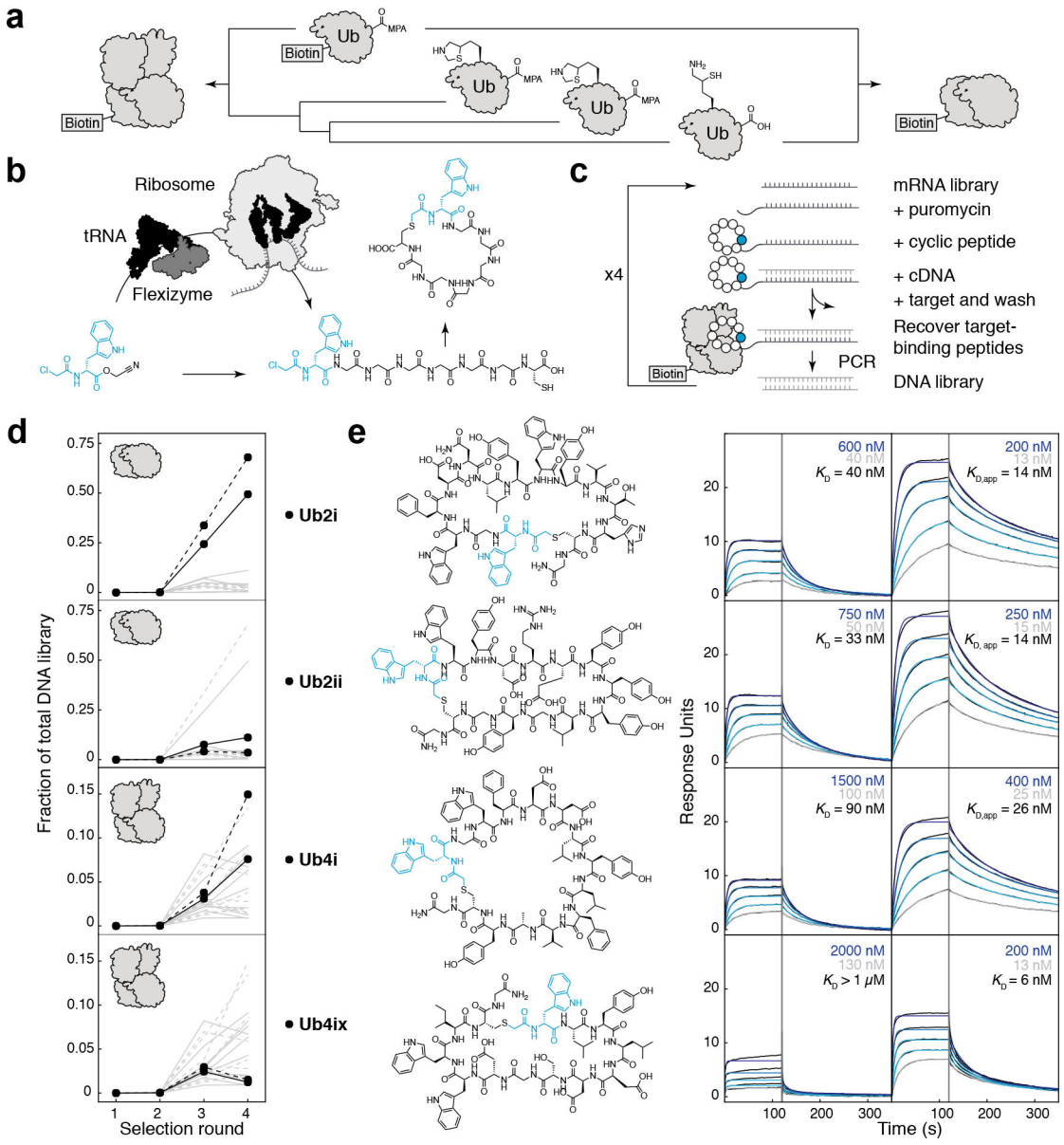

Figure 1. RaPID selection of $^{K48}Ub_n$ binding cyclic peptides.

a) Chemical synthesis of biotin-K48-linked di/tetra-Ub chain. **b**) Flexizyme, an artificial tRNA aminoacylation ribozyme, can load nonproteinogenic amino acids onto tRNA (black), for use by the ribosome in *in vitro* translation. nonproteinogenic amino acids with an N-terminal ClAc group will spontaneously react with intramolecular cysteine and can be used to form macrocyclic peptides. **c**) Large libraries (~10^{13}) of DNA-tagged cyclic peptides can be generated in the RaPID system, from which sequences can be isolated to tightly bind a protein target. **d**) Using $^{K48}Ub_2$ as a target, RaPID DNA libraries became enriched in certain peptide sequences (grey lines), with **Ub2i** and **Ub2ii** (black) as the dominant peptides (selection repeat shown as dashed lines). Using $^{K48}Ub_4$ as a target, **Ub4i** and **Ub4ix** (black) emerged amongst the enriched peptides. **e**) (top to bottom) Synthesized peptides **Ub2i**, **Ub2ii**, **Ub4i, Ub4ix** and their binding to $^{K48}Ub_2$ (left) and $^{K48}Ub_4$ (right) detected using

SPR. Highest and lowest peptide SPR concentrations are shown in blue and grey respectively.

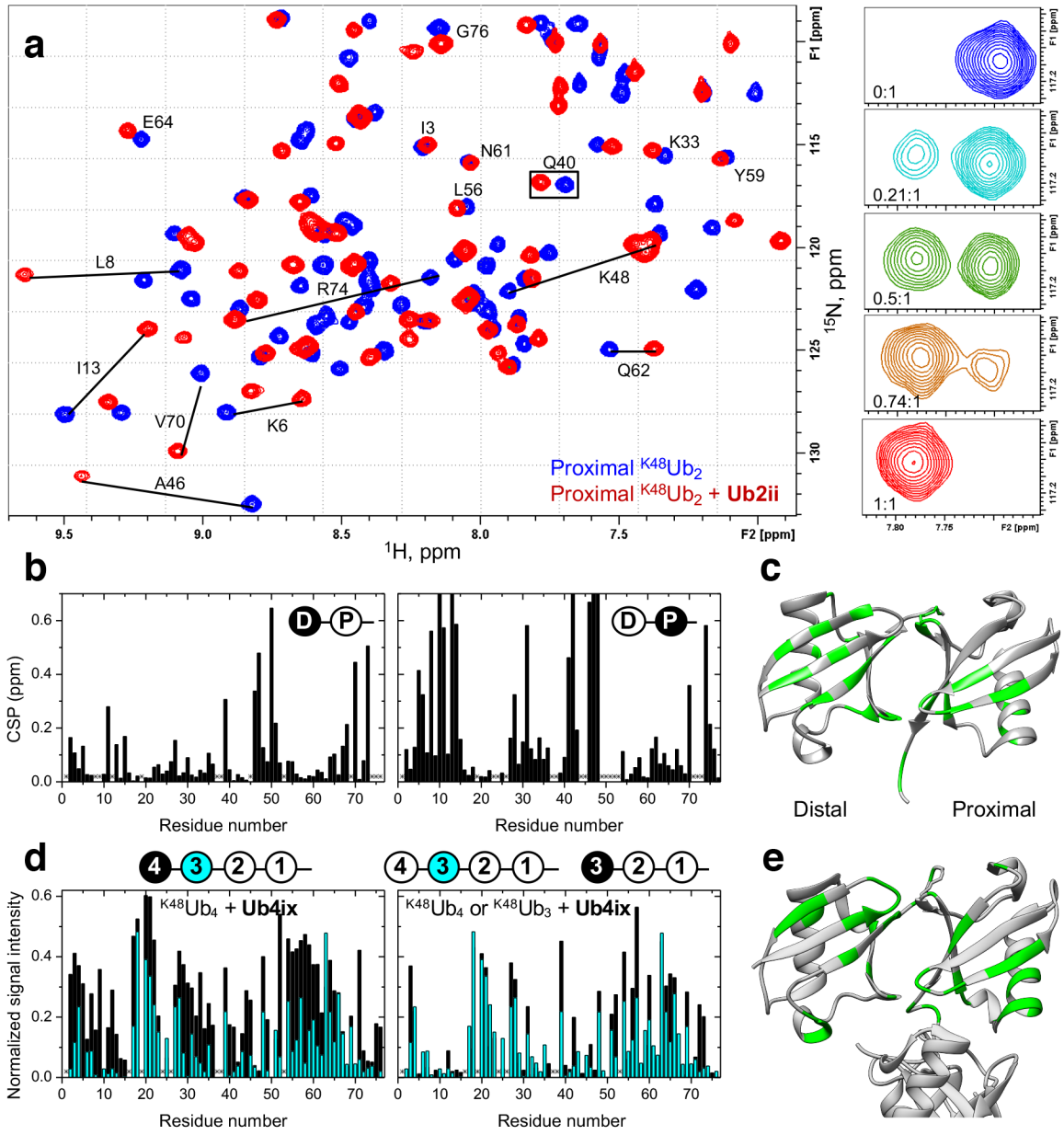

Figure 2. Cyclic peptides bind to residues at the hydrophobic Ub-Ub interface in K48-linked di- and tetra-Ub.

a) Overlay of the ^{1}H-^{15}N correlation spectra of $^{K48}Ub_2$ (proximal Ub) free (blue) and in the presence (red) of 1 molar equivalent of **Ub2ii**. Signal shifts for select residues are indicated. Insets on the right illustrate the behavior of the signal of Q40 (boxed) during the titration, at the indicated peptide:Ub_2 molar ratios. **b)** Residue-specific chemical shift perturbations (CSP) at the endpoint of titration with **Ub2ii** in the distal (left) and proximal (right) Ub units in $^{K48}Ub_2$. **c)** The perturbed residues are mapped (CSP above the mean for each domain colored green) on the crystal structure of the closed state of $^{K48}Ub_2$ (PDB 1AAR) **d)** (Left) Comparison of the intensities of the unbound signals of the most distal (unit 4, black bars) and the next to distal (unit 3, cyan bars) Ub units in $^{K48}Ub_4$ upon addition of **Ub4ix** in 2:1

and 1.5:1 molar ratio, respectively. The signal intensity for each residue was normalized to the corresponding intensity in the absence of peptide. (Right) A similar comparison of the signal intensities in $^{K48}Ub_4$ unit 3 (cyan) versus the distal Ub in $^{K48}Ub_3$ (unit 3, black), both at the 1.5:1 molar ratio (peptide:polyUb). The drawings on top indicate which Ub units in $^{K48}Ub_4$ and $^{K48}Ub_3$ are analyzed. Asterisks in (b) and (d) indicate residues that could not be detected or could not be reliably quantified due to signal overlap. **e)** Map of the residues showing strong signal attenuations (normalized signal intensity < 0.2 colored green) in the two distal Ub units (4 and 3) of $^{K48}Ub_4$ on the crystal structure of the closed form of $^{K48}Ub_4$ (PDB 2O6V).

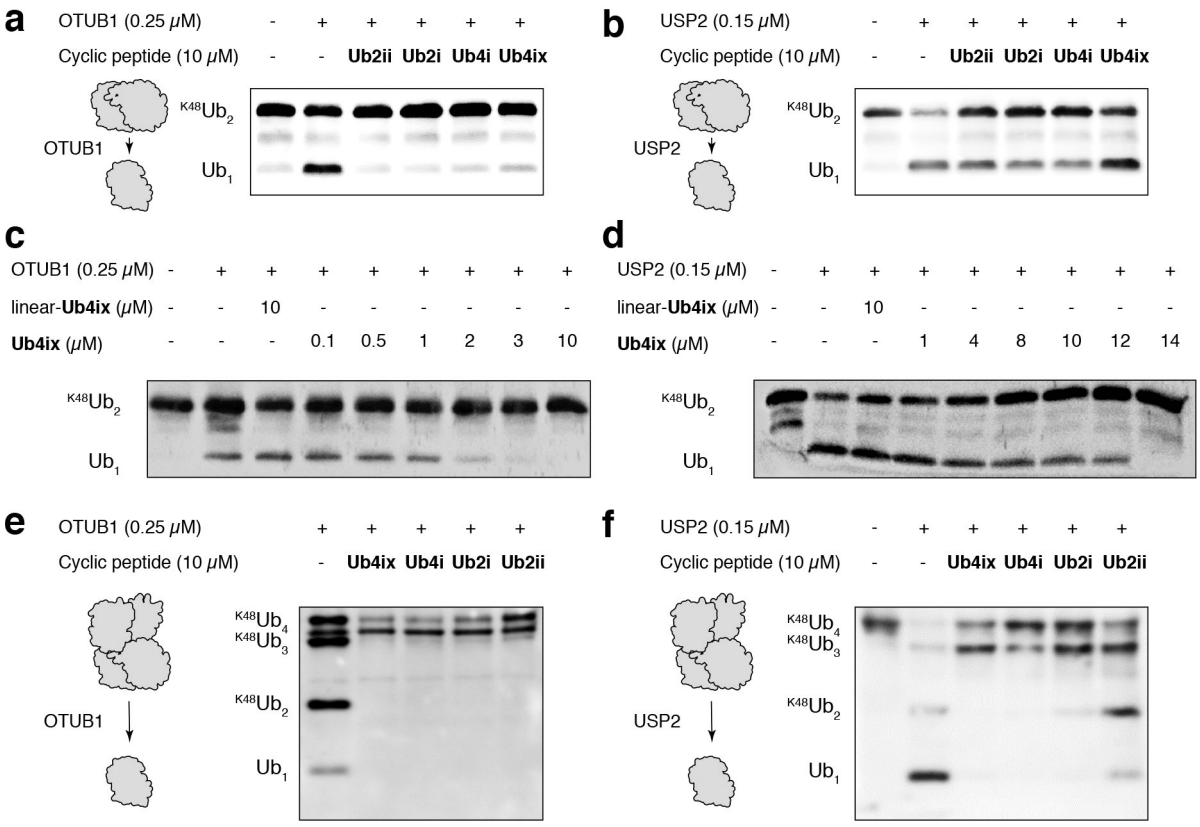

Figure 3. Cyclic peptides inhibit the DUB cleavage of K48-linked di/tetra-Ub.

a) $^{K48}Ub_2$ incubated with the K48-linked specific DUB OTUB1 for 1 hour resulted in cleavage to Ub_1. This reaction was inhibited by all cyclic peptides. **b**) $^{K48}Ub_2$ incubated with the non-linkage-specific DUB USP2 resulted in cleavage to Ub_1, cleavage could be inhibited by all peptides. **c**) **Ub4ix** inhibits OTUB1 in a dose dependent manner, with an IC_{50} approximately the same as the substrate concentration ($^{K48}Ub_2$ initially at 2 μM). **d**) Excess of **Ub4ix** (relative to $^{K48}Ub_2$ substrate) was required to fully inhibit the activity of USP2 over a 1 hour incubation. **e**) $^{K48}Ub_4$ incubated for 2 hours with OTUB1 resulted in cleavage to $^{K48}Ub_3$, $^{K48}Ub_2$ and Ub_1. In the presence of cyclic peptides, cleavage to $^{K48}Ub_3$ occurred, but further cleavage was inhibited. **f**) Similar for OTUB1, $^{K48}Ub_4$ incubated for 1 hour with USP2 could cleave to $^{K48}Ub_3$, $^{K48}Ub_2$ and Ub_1, and this cleavage was inhibited by the cyclic peptides. In all experiments, equal amounts were loaded on SDS-PAGE gel, electro-blotted to nitrocellulose membrane, and probed with an anti-Ub antibody. Initial concentrations of $^{K48}Ub_2$ or $^{K48}Ub_4$ substrate were 2 μM in each case.

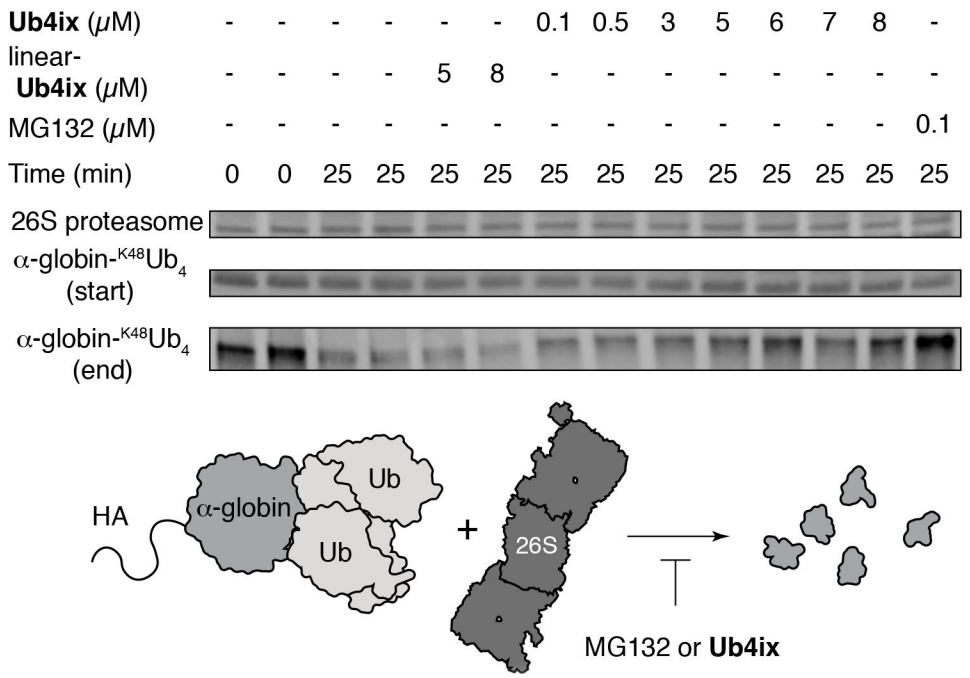

Figure 4. Ub4ix cyclic peptide inhibits 26S proteasomal activity *in vitro*.

HA-α-globin-$^{K48}Ub_4$ (5 μM) and 26S proteasome (150 nM) were combined in the presence and absence of cyclic peptide **Ub4ix**, linear-**Ub4ix** or MG132. Before and after incubation, products were separated on SDS-PAGE gel, electro-blotted and probed with anti-HA antibody. Linear-**Ub4ix** offers no protection to HA-α-globin-$^{K48}Ub_4$ from the activity of the proteasome, resulting in degradation. Cyclic peptide **Ub4ix**, at a similar concentration to the HA-α-globin-$^{K48}Ub_4$ substrate (5 μM) can protect it from degradation by the proteasome, a similar result to the adding the direct proteasome inhibitor MG132.

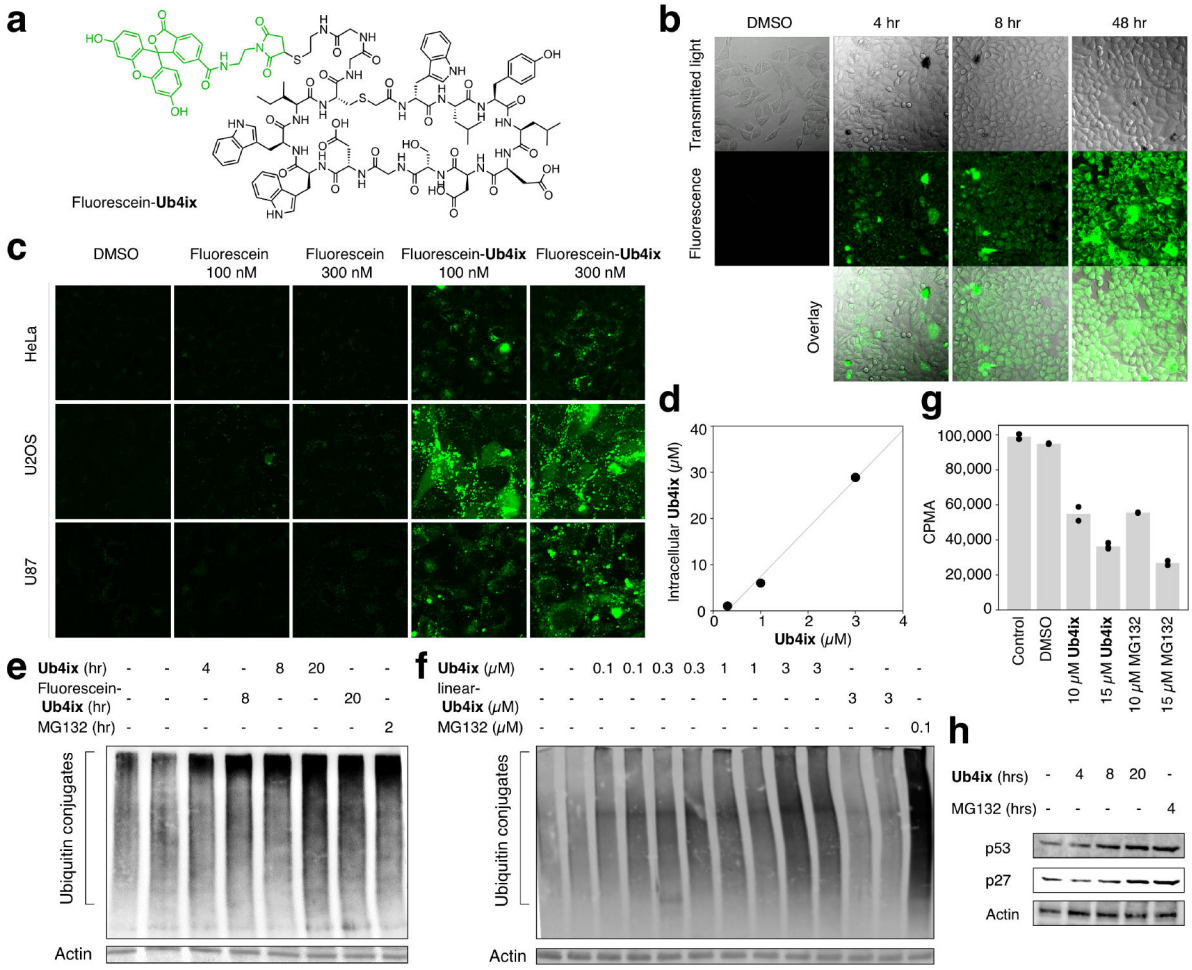

Figure 5. Uptake of Ub4ix by living cells and effect on ubiquitination.

a) Fluorescein-**Ub4ix** structure. **b**) **Ub4ix** can enter cells. HeLa cells were incubated with fluorescein-Ub4ix cyclic peptide (20 μM). Internalization of the peptide into the cells was monitored at the indicated time points. **c**) In three cell lines, HeLa, U2OS osteosarcoma and U87 primary glioblastoma cells, fluorescein-**Ub4ix** is retained in cells after washing, whereas fluorescein alone is lost. **d)** Screening of the cellular uptake fluorescein-**Ub4ix** after incubation for 16 hr shows significant retention inside cells. **e**) **Ub4ix** induced the accumulation of Ub-conjugates. HeLa cells were incubated in the presence of **Ub4ix**, Fluorescein-**Ub4ix**, or MG132 for the indicated time-periods. **f**) **Ub4ix** induced the accumulation of Ub-conjugates in a dose dependent manner. Cells were lysed, resolved using SDS-PAGE, proteins were transferred to a nitrocellulose membrane, and the membrane was blotted using an antibody against Ub-conjugates and Actin. **g**) **Ub4ix** inhibits protein breakdown inside cells. HeLa cells were labeled with radioactive ^{35}S-Met and ^{35}S-Cys, and were then chased for 4 hr in “cold” media. Cells were either non-treated, or incubated in the presence of DMSO, **Ub4ix**, or MG132. Radioactivity levels (counts per min, CPMA) from protein breakdown during the chase phase, show that **Ub4ix** and MG132 inhibit. Bars represent mean values. **h**) **Ub4ix** causes the accumulation of proteins that are normally turned over by the UPS. HeLa cells were incubated in the presence of 10 μM

Ub4ix or 10 μM MG132 for the indicated times. Cells were lysed, resolved using SDS-PAGE, proteins were transferred to a nitrocellulose membrane, and the membrane was blotted using an antibody against p53, p27 and Actin.

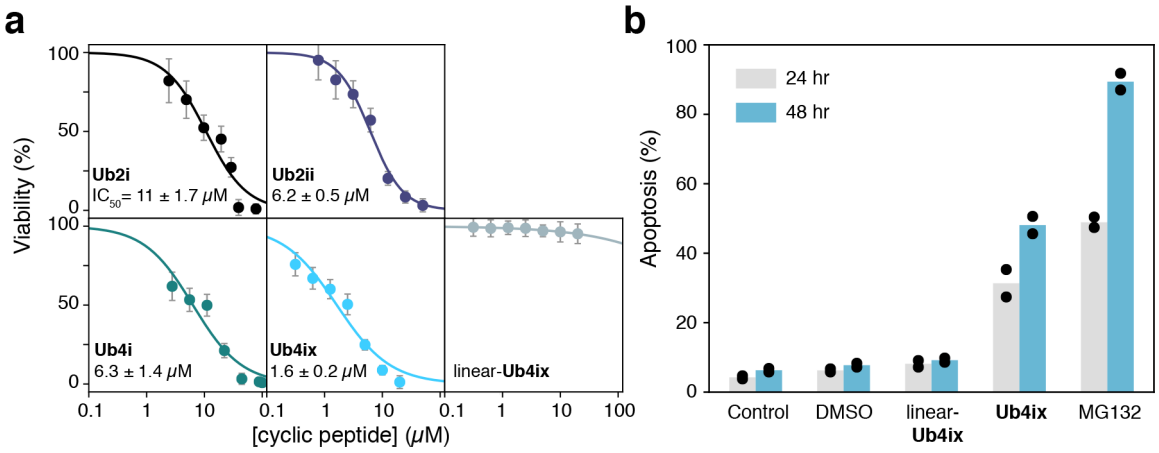

Figure 6. Ub4ix reduces cell viability and induces apoptosis.

a) Cyclic peptides reduce HeLa cells viability, as measured by MTT assay. **Ub4ix** inhibits the cell viability of HeLa cells with an IC_{50} of 1.6 μM after 48 hr incubation. Viability was measured after 72 hr for **Ub2i**, **Ub2ii, Ub4i** and linear-**Ub4ix**. Error bars represent SD of technical replicates (n=16). **b**) **Ub4ix** induces apoptosis in HeLa cells. Cells were exposed to the **Ub4ix** cyclic or linear peptide, MG132 (all at 10 μM) for 24 and 48 hr, FACS was used to follow apoptosis and cumulative cell death, bars represent mean values.